

Buckled in translation

E. Wandersman*, N. Quennouz, M. Fermigier, A. Lindner†, and O. du Roure

Laboratoire de Physique et Mécanique des Milieux Hétérogènes- UMR 7636 CNRS/ESPCI Paristech - Université Pierre et Marie Curie - Université Paris Diderot - 10, rue Vauquelin - 75005 Paris -France

We report experiments on the deformation and transport of an elastic fiber in a viscous cellular flow, namely a lattice of counter-rotative vortices. We show that the fiber can buckle when approaching a stagnation point. By tuning either the flow or fiber properties, we measure the onset of this buckling instability. The buckling threshold is determined by the relative intensity of viscous and elastic forces, the elasto-viscous number S_p . Moreover we show that flexible fibers escape faster from a vortex (formed by closed streamlines) compared to rigid fibers. As a consequence, the deformation of the fiber changes its transport properties in the cellular flow.

PACS numbers:

The interaction of a deformable body with a viscous flow is found in a wide range of situations, ranking from biology to polymer science. Cells or micro-organisms in water use deformation of high-aspect ratio flexible organelles called cilia or flagella to move at low Reynolds number [1]. Numerous studies have been dedicated to locomotion and hydrodynamic interactions at low Reynolds number, including the study of biological [2, 3] or model systems [3–8], but a large number of questions remains still to be answered. The stretching of a flexible polymer in a viscous flow is well studied [9]. The so called coil-stretch transition is responsible for the spectacular macroscopic properties of polymer solutions as for example normal stresses or high elongational viscosities. This transition might have an analog for elastic fibers that buckle by viscous forces. Microscopic buckling of fibers has indeed been shown theoretically to lead to original rheological properties of their suspensions, such as the appearance of normal stress differences [10]. An other fundamental question is the modification of the translational dynamics of an object induced by its deformation in a viscous flow as studied by Young and Shelley [11].

The complex dynamics of such systems originates from different sources: first, the dynamics is dependent on the size of the deformable body with respect to the characteristic lengthscales of the flow. Second, when the structure is deformed by viscous forces, the local surrounding flow will be modified leading to non-linear effects. Hydrodynamic interactions between flexible objects further increase complexity [12]. The experimental study of simple model systems, such as homogeneous elastic fibers, evolving in a controlled flow geometry, could help understanding these complex interactions.

In this communication we experimentally study the deformation of an isolated macroscopic filament approaching a stagnation point and the subsequent modification of its transport through a cellular flow of counter-rotating

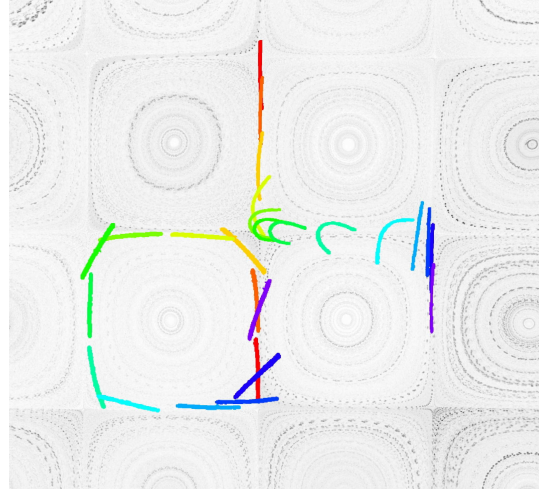


FIG. 1: Successive shapes of two fibers experiencing the same flow field but with different Young moduli ($\Delta t = 0.4s$, from red to purple). The more rigid fiber (bottom left) does not buckle whereas buckling is observed for the more flexible fiber (up right). The background flow is visualized independently.

vortices (see figure 1). First we characterize the buckling transition of the fiber varying the properties of the fiber and the viscous flow independently and identify the buckling threshold. The threshold is shown to be function of the relative intensity of the viscous and elastic forces, the so called S_p number [13]. We then discuss differences in the transport of rigid and flexible fibers in the cellular flow and show that deformation significantly changes the transport properties.

The lattice of counter-rotating vortices is obtained using electromagnetic forcing [14, 15]. An electric current is applied to an electrolyte placed in a rectangular cell (Fig. 2a). A lattice of 4x5 magnets (NdFeB, Supermagnets) with alternating orientation is placed underneath the cell, creating a spatially periodic magnetic field. Locally varying Lorentz forces act on the flowing electrolyte leading to an array of counter-rotating vortices of size $W = 3$ cm. The electrolyte is a 50:50 mixture of Polyethylenegly-

*present address: Kamerlingh Onnes Lab, Universiteit Leiden, Postbus 9504, 2300 RA, Leiden, The Netherlands

†corresponding author : anke.lindner@espci.fr

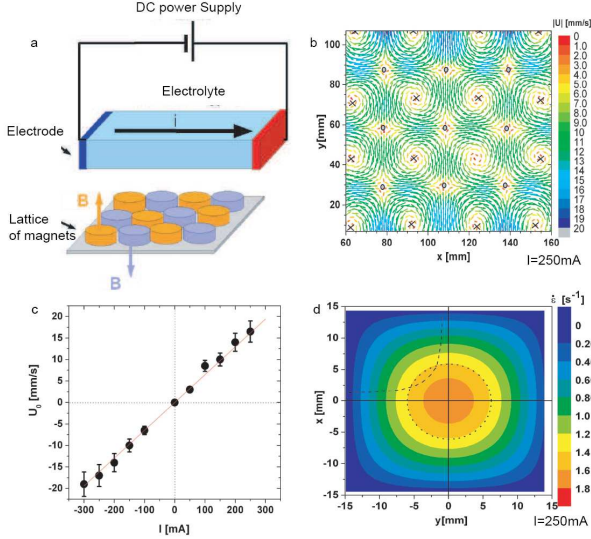


FIG. 2: a) Experimental setup: a lattice of magnet with alternated orientation is placed below an electrolyte. b) Velocity field. Closed circles represent stagnation points; crosses, centers of the vortices. c) Maximum velocity U_0 vs electric current I . The line is the best linear fit. d) Color mapping of the local compression rate ϵ in a cell. The dashed line is one experimental trajectory of the fiber. The dotted circle represents $0.8 \epsilon^{max}$.

col 1000 (Fluka) and purified water, into which NaCl is added up to saturation (viscosity, $\eta = 35 \pm 5$ mPa.s, surface tension $\gamma = 43 \pm 1$ mN/m. The electric current $I = -400/+400$ mA is applied via a DC power supply using carbon fiber electrodes (Toyobo).

The array of vortices generates a cellular flow and an array of stagnation points. Close to the stagnation points the flow can be described by hyperbolic streamlines, corresponding to a purely elongational flow with constant elongation/compression rate $\dot{\epsilon}$. Close to the center of the vortices the flow can be described by solid rotation without any deformation of the fluid. Note that the flow consists of closed streamlines and small particles can not be transported across the flow field when diffusion and particle inertia are neglected.

The velocity field is determined by Particle Imaging Velocimetry (using DAVIS software) and presented on figure 2. All our experiments are performed in a selected region, a 3×3 lattice of stagnation points, where boundary effects are negligible. The velocity field is well described by the following equation:

$$\vec{U}(\tilde{x}, \tilde{y}) = U_0 \begin{pmatrix} \sin(\tilde{x})\cos(\tilde{y}) \\ -\cos(\tilde{x})\sin(\tilde{y}) \end{pmatrix} \quad (1)$$

where \tilde{x} (resp. \tilde{y}) is the dimensionless coordinate $\pi x/W$ (resp. $\pi y/W$). \tilde{x} and \tilde{y} are set to zero at a stagnation point. The parameter U_0 is found to be proportional to the electric current I (see fig. 2c). Note that in the range of velocities used the Reynolds number is always below

5. The local compression rate of the flow reads:

$$\dot{\epsilon}(\tilde{x}, \tilde{y}, I) = \pm \frac{\pi U_0(I)}{W} \cos(\tilde{x}) \cos(\tilde{y}) \quad (2)$$

with opposite signs considering either compressive or extensive quadrants. The direction of compression remains within one quadrant always the same. The compression rate is locally variable, being maximum at the stagnation point ($\dot{\epsilon}_{max} = \pi U_0/W$), and zero at the center of the vortices.

During its motion in the lattice, a fiber thus experiences a variable compression rate $\dot{\epsilon}(\tilde{x}, \tilde{y})$. This is illustrated in figure 2d, where the local compression rate is color mapped in a cell centered on a stagnation point. All our experimental trajectories reach 80% of $\dot{\epsilon}_{max}$. Thus, for sake of simplicity, we will hereafter use this value to characterize the flow influence.

Experiments are performed with macroscopic fibers (length $L = 12 \text{ mm} \pm 0.5 \text{ mm}$, radius $r = 85 \pm 5 \mu\text{m}$) made by crosslinking vinylpolysiloxane with a curing agent (Zhermack, 8 Shore A) in a glass capillary. The filament is then carefully extruded from the capillary. Optical measurements on a microscope have been used to measure the radius of the fiber as well as to verify that it is homogeneous and not damaged over the whole length. The ratio between its length and the cell size $\alpha = L/W = 0.4$ is fixed for all experiments. The mass ratio between the curing agent and the polymer can be varied from 1:2 to 3:1. The Young's modulus is obtained via rheological measurements using $Y = 3G'$ and can be tuned from $Y = 75 \text{ kPa}$ to $Y = 180 \text{ kPa}$.

The density of the fiber is lower than the density of the fluid ($\Delta\rho = 0.15 \cdot 10^3 \text{ kg/m}^{-3}$) and the fiber thus floats at the surface. More precisely, the equilibrium position of the fiber at the interface is determined by the interplay between gravity and surface tension [16]. For our system, surface tension dominates, leading to the absence of a meniscus. The degree of immersion of the fiber is then solely controlled by the wetting angle between the liquid and the fiber. We find this angle to be $90 \pm 5 \text{ deg}$ and the fiber is approximatively half-immersed. As a consequence, the motion as well as the deformation of the fiber are bidimensional, constrained at the surface of the flow. As the interface is not deformed, the influence of surface tension on the dynamics of the filament is negligible.

Pictures of the fiber are taken with a digital camera (PixelLink, 1024x768, 10 fps). Using standard detection procedures (ImageJ software), we measure the position of the center of mass of the fiber. A fit of the shape is performed with spline functions (Numerical Recipes 3.3), and used to extract the mean curvature of the fiber as a function of time t , $C(t)$.

We will now use the experimental set-up to study the buckling instability of the flexible fibers in the vicinity of a stagnation point. Figure 1 shows two typical trajectories of a fiber with different elastic moduli, but evolving in the same flow. One observes that the rigid fiber does

not buckle when approaching the stagnation point, the flexible fiber however is deformed by the flow and shows a buckling instability.

To characterize this buckling instability in detail we construct the probability of a fiber to buckle in a given flow. We consider trajectories of the fiber cell by cell, where a cell is a square of width W , centered on a stagnation point. One trajectory is defined as the path in the vicinity of one stagnation point as illustrated by the dashed line on figure 2d. The fiber is said in "coiled state" if the mean curvature is larger than a given threshold $C_{coil} = 0.125 \text{ mm}^{-1}$, i.e. to a radius of curvature of approximatively $2L/3$. This corresponds to almost a quarter of a circle. No quantitative modifications of the results are observed if the threshold is slightly tuned. We do not consider trajectories where the filament enters the cell in a coiled state. We determined, for each experiment the ratio between the number of trajectories displaying a coiled state N_{coiled} and the total number of trajectories N_{tot} . Assembling over 20 experiments, around 7000 trajectories of the fiber are considered, with a total number of buckling events equal to ≈ 500 .

The fiber is predicted to buckle when viscous forces overcome elastic forces. Their relative intensity is given by the Sperm number S_p [13]:

$$S_p = \frac{\eta \dot{\epsilon} L^4}{Y r^4}. \quad (3)$$

Our set-up allows to vary the properties of the fiber and of the viscous flow separately tuning the two forces independently. The inset of figure 3 shows the probability to buckle as a function of the maximum velocity of the flow U_0 for different Young's moduli ($Y=75, 120$ and 180 kPa). One observes for all cases an increase with U_0 . One observes furthermore that the probability to buckle is higher for the flexible fibers.

Figure 3 now shows the probability to buckle for all experiments and its average as a function of S_p . Within the experimental resolution the data points fall on a single curve, showing that the S_p number is indeed the control parameter of the system, as predicted by Young *et al.* [11].

The probability to buckle is zero below $S_p = 120$, it increases at $S_p \sim 120 - 150$ and reaches at our highest S_p about 20%. Theoretical predictions from linear stability analysis in a hyperbolic flow show a threshold of $S_p^* = 153$ for the buckling instability [17] [11]. Note that their definition of S_p^* includes the logarithmic correction from slender body theory and reads $S_p^* = \frac{16\eta \dot{\epsilon}}{Y(\ln(L/R)-1/2)} \frac{L^4}{r^4}$. We correct the experimentally obtained value for the buckling threshold in the same way and find $S_p^* \sim 400$. In the experiments the fibers are only half-immersed and viscous forces are certainly smaller than those used in the theoretical analysis. This is likely to be the main reason for the higher threshold observed in our experiments. Furthermore, even if we only consider filaments passing close to the stagnation point, the filament is of

significant length compared to the typical lengthscale W of the cellular flow and the approximation of hyperbolic streamlines does not hold in our experiments.

We do not observe an abrupt increase of the probability towards 100% at the threshold but a continuous increase with S_p . At the highest value of S_p accessible in our experiments the filament still only buckles one out of four times it passes a stagnation point. This indicates that even if the threshold of buckling is controlled by S_p the dynamics in the cellular flow are more complicated. It is likely that the probability might increase further when going to higher values of S_p .

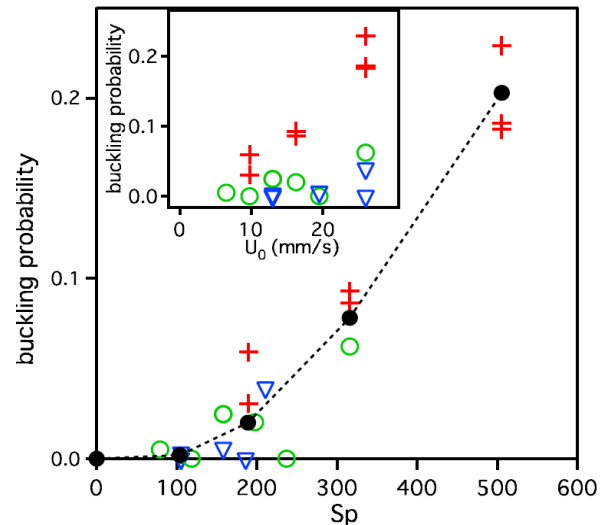


FIG. 3: Probability of buckling vs S_p for different Young moduli (red cross $Y=75$ kPa, blue triangle $Y=120$ kPa, green open circle $Y=180$ kPa). Black closed circles represent the mean value. Inset: Probability of buckling as a function of U_0 .

With our experiment we can also address an other fundamental question which stands in the modification of the translational dynamics of the filament induced by its deformation. To do so we study the escape of a filament from a vortex. The finite size of the fiber already changes its dynamics in the cellular flow compared to a pointlike particle (see figure 1). We will thus compare deformable fibers ($S_p > 120$) to rigid fibers ($S_p < 120$). The fibers are placed in a vortex parallel to the axis of compression and at a given distance b (see figure 4c). We then record the number of trajectories the filament needs to escape from the vortex and the number of buckling events during this escape for over 250 experiments.

Figure 4 shows the number of trajectories as well as their average above and below the buckling threshold $S_p = 120$ as a function of b normalized by the size of the vortex $W/2$. Note that the range of b studied corresponds to trajectories of the filament reaching at least 80 % of the maximum compression rate, identical to the experiments used to study the buckling probability.

Trivially, one observes that the filament needs longer

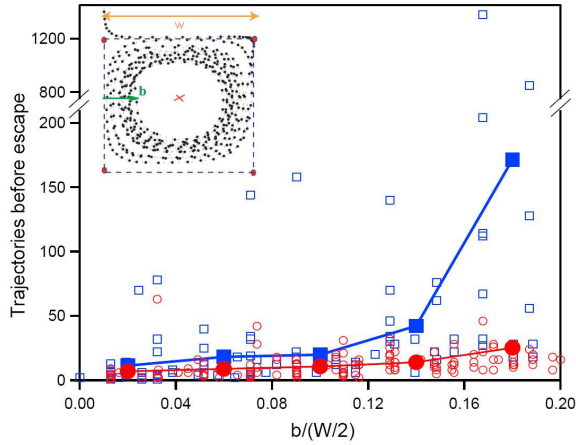


FIG. 4: Number of trajectories before escape as a function of $b/(W/2)$. Open symbols, individual experiments; closed symbols, the mean value. Red circles $S_p > 120$, blue squares $S_p < 120$. Inset, definition of b .

to escape from a vortex if it is further away from the axis of compression. One observes also that even the rigid filaments escape from the vortices after a finite number of trajectories, showing the importance of the effect of the finite size of the filament. The number of trajectories needed to escape from a vortex fluctuates strongly in the case of the rigid fibres, indicating that small changes in the initial position (not measured in this analysis) are important for the dynamics. Less fluctuations are observed for the flexible filaments. When comparing the average number of trajectories of the flexible fibers and the rigid fibers one observes that the flexible filaments escape significantly faster. This is a clear signature of the effect of the filament's deformation on its transport properties.

Young and Shelley show that the onset of the buck-

ling instability is coupled to the onset of a translational "Brownian like" motion of the fiber across the lattice of stagnation points [11]. Above the stretch coil transition, fibers present a diffusive behavior, with however, a non trivial dependence of the diffusion coefficient with the relative intensity of viscous and elastic forces. The motion of a fiber in one cell can be seen as a 'collision' with the stagnation point. Sequences of these collisions can then lead to diffusion of a fiber. Our results are the first indication that flexible fibers indeed diffuse faster than rigid ones through the cellular flow.

In conclusion, we have built an experimental setup allowing to study the deformation and the transport of a centimetric fiber in a cellular flow, formed by counter-rotating vortices. We have shown that the elastic fiber can buckle due to the compressive viscous forces. We have identified the threshold for the buckling instability, which is function of the so called S_p number, being a measure of the relative intensity of viscous and elastic forces. These experimental observations are in reasonable agreement with linear stability analysis in a purely hyperbolic flow. We have also studied the translational dynamics of the filament in the cellular flow field. We have shown experimentally that fibers can escape from a given vortex due to their finite size compared to the size of the vortex. Flexible fibers are shown to escape after significantly less tours compared to rigid fibers. This is a first evidence that the deformation of a filament changes its transport properties in the cellular flow.

We thank Mike Shelley for having initiated and closely followed this study. We have benefitted from many enlightening discussions with him. We thank Yuan-Nan Young, Olivier Cardoso and Denis Bartolo for fruitful discussions. We acknowledge Jose Lanuza for supporting us in the construction of the set-up and Guylaine Ducouret for help with the rheological measurements.

-
- [1] D. Bray. *Cell Movements: From Molecules to Motility*. Taylor & Francis. Garland, N.Y., 2001.
 - [2] Marco Polin, Idan Tuval, Knut Drescher, J. P. Gollub, and Raymond E. Goldstein. Chlamydomonas Swims with Two "Gears" in a Eukaryotic Version of Run-and-Tumble Locomotion. *Science*, 325(5939):487–490, 2009.
 - [3] Manouk Abkarian and Annie Vialat. Swinging of red blood cells under shear flow. *Phys. Rev. Lett.*, 98:188302, 2007.
 - [4] N. Coq, O. du Roure, J. Marthelot, D. Bartolo, and M. Fermigier. Rotational dynamics of a soft filament: Wrapping transition and propulsive forces. *Physics of Fluids*, 20(5):051703, 2008.
 - [5] Bian Qian, Thomas R. Powers, and Kenneth S. Breuer. Shape transition and propulsive force of an elastic rod rotating in a viscous fluid. *Phys. Rev. Lett.*, 100(7):078101, 2008.
 - [6] Tony S. Yu, Eric Lauga, and A. E. Hosoi. Experimental investigations of elastic tail propulsion at low Reynolds number. *Physics of Fluids*, 18(9):091701, 2006.
 - [7] R. Dreyfus, J. Baudry, M. L. Roper, M. Fermigier, H. A. Stone, and J. Bibette. Microscopic artificial swimmers. *Nature*, 437(7060):862–865, Oct 2005.
 - [8] A. Snezhko, M. Belkin, I. S. Aranson, and W.-K. Kwok. Self-assembled magnetic surface swimmers. *Phys. Rev. Lett.*, 102(11):118103, Mar 2009.
 - [9] Thomas T. Perkins, Douglas E. Smith, and Steven Chu. Single Polymer Dynamics in an Elongational Flow. *Science*, 276(5321):2016–2021, 1997.
 - [10] L.E. Becker and M.J. Shelley. Instability of elastic filaments in shear flow yields first-normal-stress differences. *Phys. Rev. Lett.*, 87:198301, 2001.
 - [11] Y.N. Young and M.J. Shelley. Stretch-coil transition and transport of fibers in cellular flows. *Phys. Rev. Lett.*, 99:058303, 2007.
 - [12] Y.N. Young. Hydrodynamic interactions between two

- semiflexible inextensible filaments in stokes flow. *Phys. Rev. E*, 79:046317, 2009.
- [13] Chris H. Wiggins and Raymond E. Goldstein. Flexive and propulsive dynamics of elastica at low reynolds number. *Phys. Rev. Lett.*, 80(17):3879–3882, Apr 1998.
 - [14] O. Cardoso, D. Marteau, and P. Tabeling. Quantitative experimental study of the free decay of quasi-two-dimensional turbulence. *Phys. Rev. E*, 49(1):454–461, Jan 1994.
 - [15] M. J. Twardos, P. E. Arratia, M. K. Rivera, G. A. Voth, J. P. Gollub, and R. E. Ecke. Stretching fields and mixing near the transition to nonperiodic two-dimensional flow. *Phys. Rev. E*, 77:056315, 2008.
 - [16] A. V. Rapacchietta, A.W. Neumann, and S.N. Omenyi. Force and free-energy analyses of small particles at fluid interfaces. *Journal of Colloid and Interface Science*, 59:541, 1977.
 - [17] Mike Shelley, Private communication, 2009